

Small grid embeddings of 3-polytopes

Ares Ribó Mor*

Günter Rote†

André Schulz‡

November 4, 2018

Abstract

We introduce an algorithm that embeds a given 3-connected planar graph as a convex 3-polytope with integer coordinates. The size of the coordinates is bounded by $O(2^{7.55n}) = O(188^n)$. If the graph contains a triangle we can bound the integer coordinates by $O(2^{4.82n})$. If the graph contains a quadrilateral we can bound the integer coordinates by $O(2^{5.46n})$. The crucial part of the algorithm is to find a convex plane embedding whose edges can be weighted such that the sum of the weighted edges, seen as vectors, cancel at every point. It is well known that this can be guaranteed for the interior vertices by applying a technique of Tutte. We show how to extend Tutte’s ideas to construct a plane embedding where the weighted vector sums cancel also on the vertices of the boundary face.

1 Introduction

Problem Setting. The graph of a polytope is an abstraction from its geometric realization. For a 3-polytope, the graph determines the complete combinatorial structure. The graphs of 3-polytopes are characterized by Steinitz’ seminal theorem [31], which asserts that they are exactly the planar 3-connected graphs.

A natural question is to ask for a geometric realization of a 3-polytope when its combinatorial structure is given. One might be interested in a realization that fulfills additionally certain optimality criteria. For example a good resolution is desirable to obtain aesthetic drawings [6, 30]. We address a different problem and ask for an embedding whose vertices can be placed on a small integer grid. The vertex coordinates of such an embedding can be stored efficiently.

Related Work. Suppose we are given the combinatorial structure of a 3-polytope by a graph G with n vertices. The original proof of Steinitz’ theorem transforms the 3-connected planar graph G into the graph of the tetrahedron by a sequence of elementary operations. The transformation preserves the realizability as a 3-polytope. Since all operations can be carried out in the rationals, the proof gives a method to construct a realization of a 3-polytope with integer coordinates. However, it is not easy to keep track of the size and the denominators of the coordinates, which makes it difficult to apply this approach for our problem. An alternative proof of Steinitz’ theorem goes back to the Koebe-Andreev-Thurston Circle Packing Theorem (see for example Schramm [28]). This approach relies on non-linear methods, which make the (grid) size of the embedding intractable. A third proof of Steinitz’ theorem relies on the “liftability” of planar barycentric embeddings. Since this *barycentric approach* is based on linear methods, its construction favors computational aspects

*Gesellschaft zur Förderung angewandter Informatik e.V., Berlin, Germany, ribo@gfai.de. Partially supported by the Deutsche Forschungsgemeinschaft within the European Research Training Network *Combinatorics, Geometry and Computation* (No. GRK 588/2).

†Institut für Informatik, Freie Universität Berlin, Germany, rote@inf.fu-berlin.de.

‡Institut für Mathematische Logik und Grundlagenforschung, Universität Münster, andre.schulz@uni-muenster.de. Partially supported by the German Research Foundation (DFG) under grant SCHU 2458/1-1.

of the embedding. This led to a series of embedding algorithms: Hopcroft and Kahn [14], Onn and Sturmfels [20], Eades and Garvan [12], Richter-Gebert [24], Chrobak, Goodrich, and Tamassia [6]. Our work also follows this paradigm.

As a first quantitative analysis of Steinitz' theorem, Onn and Sturmfels [20] showed that integer coordinates smaller than n^{169n^3} suffice to realize a 3-polytope. Richter-Gebert improved this bound to $O(2^{18n^2})$. A more careful analysis of Richter-Gebert's approach shows that the size of the integer coordinates can be bounded by 2^{12n^2} [21].

Integer realizations with at most exponentially large coordinates in terms of n were previously known for polytopes whose graph contains a triangle (Richter-Gebert [24]). We describe this method in Section 3.1 (p. 8) as Case 1 of our embedding algorithm. In Richter-Gebert's approach (and already in Onn and Sturmfels [20]), graphs without triangles are embedded by first embedding the polar polytope, whose graph in this case has to contain a triangle. Based on the polar, an embedding of the original polytope is constructed. However, this operation yields coordinates with a quadratic term in the exponent.

For *triangulated* 3-polytopes, Das and Goodrich [10] showed that they can be embedded with coordinates of size $2^{O(n)}$, using an incremental method which can be carried out in $O(n)$ arithmetic operations. Triangulated 3-polytopes are easier to realize on the grid than general polytopes, since each vertex can be perturbed within some small neighborhood while maintaining the combinatorial structure of the polytope. An explicit bound on the coordinates has not been worked out by the authors. For stacked polytopes a better upper bound exists [38], but it is still exponential.

Lower Bounds. Little is known about the lower bound of a grid embedding of a 3-polytope. An integral convex embedding of an n -gon in the plane needs an area of $\Omega(n^3)$ [1, 2, 32, 35]. Therefore, realizing a 3-polytope with an $(n - 1)$ -gonal face requires at least one dimension of size $\Omega(n^{3/2})$.

Two Dimensions. In the plane, planar 3-connected graphs can be embedded on a very small grid. For a crossing-free straight-line embedding an $O(n) \times O(n)$ grid is sufficient [11, 27]. This is also true if the embedding has to be convex [4]. A strictly convex drawing can be realized on an $O(n^2) \times O(n^2)$ grid [3].

Higher Dimensions. Already in dimension 4, there are polytopes that cannot be realized with rational coordinates, and a 4-polytope that can be realized on the grid might require coordinates that are doubly exponential in the number of its vertices. Moreover, it is NP-hard to even decide if a lattice is a face lattice of a 4-polytope [24, 25].

Results. In this article we develop an algorithm that realizes G as a 3-polytope with integer coordinates not greater than $O(187.13^n) = O(2^{7.55n})$. This implies that for any 3-polytope a combinatorially equivalent polytope can be stored with $O(n)$ bits per vertex. For the case that G contains a triangle we show that G admits an integer realization with no coordinate larger than $O(28.4^n) = O(2^{4.82n})$, if G contains a quadrilateral face, the size of the coordinates can be bounded by $O(43.99^n) = O(2^{5.46n})$. The most difficult part of the algorithm is to locate the boundary face of the plane embedding such that a lifting into \mathbb{R}^3 exists. This problem can be reduced to a non-linear system which is most complex when G contains neither a triangle nor a quadrilateral face.

Partial results containing the essential ideas for graphs with quadrilateral faces (Case 2 of Section 3.1) were presented by the second author at the workshop *The Future of Discrete Mathematics* at Štířín Castle, Czech Republic, in May 1997. The results of this paper were presented in a different form at the 23rd Annual Symposium on Computational Geometry in Gyeongju, Korea, in June 2007 [22]. Since then, we were able to simplify the computation of the explicit bounds with help of Lemma 3.10. The simplification yields slightly different bounds. By improving the bound of Lemma 9 in [22] by a polynomial factor (now Lemma 3.9) we obtain better bounds in the end.

However, our analysis could be further improved with help of the more complicated construction of [22]. Since the improvement would only result in a constant factor we decided to present the simpler and more elegant analysis.

A follow-up work [30] extends the techniques of this article and studies more general barycentric embeddings. With help of these modifications, a grid embedding with x -coordinates smaller than $2n$ can be constructed. The small x -coordinates are realized at the expense of the size of the y and z -coordinates, which are bounded by $2^{O(n^2 \log n)}$.

Remark: Most recently, Buchin and Schulz [5] improved the upper bound for the maximum number of spanning trees contained in a planar graph. This has a direct consequence for our results, since we obtain the bound for the necessary grid size in terms of this quantity. In particular, the new bounds of [5] yield that our algorithm requires a grid of size $O(147.71^n) = O(2^{7.21n})$ (general case), $O(39.87^n) = O(2^{5.32n})$ (G contains a quadrilateral face), and $O(27.94^n) = O(2^{4.81n})$ (G contains a triangular face).

2 Lifting Planar Graphs

Let $G = (V, E)$ be a 3-connected planar graph with vertex set $V = \{v_1, \dots, v_n\}$ embedded in the plane with straight edges and no crossings. The coordinates of a vertex v_i in the (plane) embedding are called $\mathbf{p}_i := (x_i, y_i)^T$, the whole embedding is denoted as $G(\mathbf{p})$. Let $h: V \rightarrow \mathbb{R}$ be a height assignment for the vertices in G . We write z_i for $h(v_i)$. If the vertices (x_i, y_i, z_i) of every face of G lie on a common plane, we call the height assignment h a *lifting* of $G(\mathbf{p})$.

Definition 1 (Equilibrium, Stress). *An assignment $\omega: E \rightarrow \mathbb{R}$ of scalars (denoted as $\omega(i, j) = \omega_{ij} = \omega_{ji}$) to the edges of G is called a stress.*

1. *A vertex v_i is in equilibrium in $G(\mathbf{p})$, if*

$$\sum_{j: (i, j) \in E} \omega_{ij} (\mathbf{p}_i - \mathbf{p}_j) = \mathbf{0}. \quad (1)$$

2. *The embedding $G(\mathbf{p})$ is in equilibrium if all vertices are in equilibrium.*
3. *If $G(\mathbf{p})$ is in equilibrium for the stress ω , then ω is called an equilibrium stress for $G(\mathbf{p})$.*

It is well known that equilibrium stresses and liftings are related. Maxwell observed in the 19th century that there is a correspondence between embeddings with equilibrium stress and projections of 3-dimensional polytopes [19]. There are different versions of Maxwell's theorem. For the scope of this article the following formulation is the most suitable.

Theorem 2.1 (Maxwell, Whiteley). *Let G be a planar 3-connected graph with embedding $G(\mathbf{p})$ and designated face f_1 . There exists a correspondence between*

- A) *equilibrium stresses ω on $G(\mathbf{p})$,*
- B) *liftings of $G(\mathbf{p})$ in \mathbb{R}^3 , where face f_1 lies in the xy -plane.*

The proof that A induces B (which is the important direction for our purpose) is due to Walter Whiteley [36]. The Maxwell-Cremona correspondence finds interesting applications in different areas (see for example Hopcroft and Kahn [14], and Connelly, Demaine and Rote [7]).

To describe a lifting, we have to specify for each face f_i of the graph the plane H_i on which it lies. We define H_i by the two parameters \mathbf{a}_i and d_i . The plane H_i is characterized by the function that assigns to every point \mathbf{p} in the plane a third coordinate by

$$H_i: \mathbf{p} \mapsto \langle \mathbf{p}, \mathbf{a}_i \rangle + d_i. \quad (2)$$

Here, $\langle \cdot, \cdot \rangle$ denotes the dot product. The correspondence between liftings and stresses comes from the observation that the “slope difference” $\mathbf{a}_l - \mathbf{a}_r$ between two adjacent faces f_l and f_r is perpendicular to the edge $\mathbf{p}_i - \mathbf{p}_j$ that separates them:

$$\mathbf{a}_l - \mathbf{a}_r = \omega_{ij}(\mathbf{p}_i - \mathbf{p}_j)^\perp, \quad (3)$$

for some scalar $\omega_{ij} \in \mathbb{R}$. Here, $\mathbf{p}^\perp := \begin{pmatrix} -y \\ x \end{pmatrix}$ denotes the vector $\mathbf{p} = \begin{pmatrix} x \\ y \end{pmatrix}$ rotated by 90 degrees. It is not hard to show that these numbers ω_{ij} form an equilibrium stress.

The other direction, the computation of the lifting of $G(\mathbf{p})$ induced by ω is straightforward, see Crapo and Whiteley [9]. We follow the presentation of Connolly, Demaine and Rote [7] for the computation of the lifting.

The parameters \mathbf{a}_i and d_i can be computed by the following iterative method: We pick f_1 as the face that lies in the xy -plane, and set $\mathbf{a}_1 = \begin{pmatrix} 0 \\ 0 \end{pmatrix}$ and $d_0 = 0$. Then we lift the remaining faces one by one. This is achieved by selecting a face f_l that is incident to an already lifted face f_r . Let (i, j) be the common edge of f_l and f_r . Assume that in $G(\mathbf{p})$ the face f_l lies left of the directed edge ij , and f_r lies right of it. The parameters of H_l can be computed by

$$\mathbf{a}_l = \omega_{ij}(\mathbf{p}_i - \mathbf{p}_j)^\perp + \mathbf{a}_r, \quad (4)$$

$$d_l = \omega_{ij} \langle \mathbf{p}_i, \mathbf{p}_j^\perp \rangle + d_r. \quad (5)$$

The formula (4) comes directly from (3), and (5) comes from the fact that the two planes must intersect above \mathbf{p}_i and \mathbf{p}_j .

The sign of the stresses allows us to say something about the curvature of the lifted graph. According to (3) and (4), the sign of ω_{ij} that separates f_l and f_r tells us if the lifted face f_l lies below or above H_r . As a consequence we obtain the following:

Proposition 1. *Let $G(\mathbf{p})$ be a straight-line embedding of a planar 3-connected graph G with equilibrium stress. If the stresses on the boundary edges are negative and all other stresses positive then the lifting induced by such equilibrium stress results in a convex 3-polytope.*

Lemma 2.1. *If $G(\mathbf{p})$ has integer coordinates only and the equilibrium stress is integral on all interior edges, then the z -coordinates of the lifted embedding are also integers.*

Proof. We select an interior face as face f_1 . The gradient $\mathbf{a}_1 = (0, 0)^T$ and the scalar $d_1 = 0$ are clearly integral. For all other interior faces f_i the parameters \mathbf{a}_i , d_i of the planes H_i can be computed with help of equations (4) and (5). By an inductive argument these parameters are integral as well. Computing the z -coordinate of some point \mathbf{p}_i by (2) boils down to the multiplication and addition of integers. \square

3 The Grid Embedding Algorithm

3.1 The Plane Embedding

The embedding of G as a 3-polytope uses the following high level approach. First we embed G in the plane, such that it is liftable (see Section 2), then we lift the embedding to \mathbb{R}^3 , finally we scale to obtain integer coordinates as described in Section 3.2. The analysis of the algorithm in Section 3.3 gives the new upper bound. The most challenging part is to construct a liftable 2d-embedding.

An embedding is called *barycentric* if every vertex that is not on the outer face is in the barycenter of its neighbors. Tutte showed that for planar 3-connected graphs the barycentric embedding for a fixed convex outer face is unique [33, 34]. Moreover, if embedded with straight lines, no two edges cross, and all faces are realized as convex polygons. In the barycentric embedding all vertices that are not on the outer face are in equilibrium according to the stress $\omega \equiv 1$. Our embedding

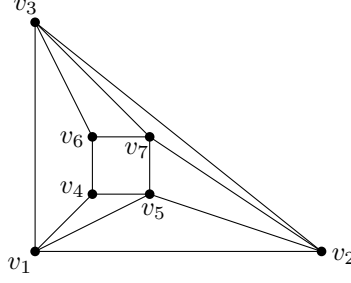


Figure 1: A small example graph.

algorithm uses this special stress only, although we state the lemmas as general as possible. Since our techniques might find applications in other settings we develop our main tools for arbitrary stresses. (Note that Tutte's approach works with arbitrary stresses that are positive on interior edges, see for example Gortler *et al.* [13].)

We describe now how to compute the barycentric embedding of G . Let f_0 be a face of G that we picked as the outer face, and let k be the number of vertices in f_0 . For simplicity we want k as small as possible. Euler's formula implies that every planar and 3-connected graph has a face f_0 with $k \leq 5$ edges. We assume that the vertices in G are labeled such that the first k vertices belong to f_0 in cyclic order. Let $B := \{1, \dots, k\}$ be the index set of the boundary vertices and let $I := \{k+1, \dots, n\}$ denote the index set of the interior vertices. The edges of f_0 are called *boundary edges*, all other edges *interior edges*. The stresses on the exterior edges will be defined later, but since they don't matter for the barycentric embedding we set them to zero for now.

We denote with $L = (l_{ij})$ the *Laplacian* matrix of G (short *Laplacian*), which is defined as follows

$$l_{ij} := \begin{cases} -\omega_{ij} & \text{if } (i, j) \in E \text{ and } i \neq j, \\ \sum_{(i,j) \in E} \omega_{i,j} & \text{if } i = j, \\ 0 & \text{otherwise.} \end{cases}$$

For the special "weights" $\omega \equiv 1$ the Laplacian equals the negative adjacency matrix of G with vertex degrees on the diagonal. We subdivide L into block matrices indexed by the sets I and B , and obtain L_{IB} , L_{BI} , L_{BB} , and L_{II} . The matrix L_{II} is called the *reduced Laplacian matrix* of G . For convenience we write \bar{L} instead of L_{II}

Example. Consider the graph of Figure 1, with $B = \{1, 2, 3\}$ and $I = \{4, 5, 6, 7\}$. We have

$$L = \left(\begin{array}{ccc|cccc} 2 & 0 & 0 & -1 & -1 & 0 & 0 \\ 0 & 2 & 0 & 0 & -1 & 0 & -1 \\ 0 & 0 & 2 & 0 & 0 & -1 & -1 \\ \hline -1 & 0 & 0 & 3 & -1 & -1 & 0 \\ -1 & -1 & 0 & -1 & 4 & 0 & -1 \\ 0 & 0 & -1 & -1 & 0 & 3 & -1 \\ 0 & -1 & -1 & 0 & -1 & -1 & 4 \end{array} \right) = \begin{pmatrix} L_{BB} & L_{BI} \\ L_{IB} & L_{II} \end{pmatrix}, \text{ with } \bar{L} = L_{II} = \begin{pmatrix} 3 & -1 & -1 & 0 \\ -1 & 4 & 0 & -1 \\ -1 & 0 & 3 & -1 \\ 0 & -1 & -1 & 4 \end{pmatrix}.$$

In the example the presence of the boundary edges $(1, 2)$, $(1, 3)$, and $(2, 3)$ is not reflected in the Laplacian, because the stress is set to zero on the boundary.

The location of the boundary vertices is given by the vectors $\mathbf{x}_B = (x_1, \dots, x_k)^T$ and $\mathbf{y}_B = (y_1, \dots, y_k)^T$. Since every vertex should lie at the (weighted) barycenter of its neighbors, the coordinates of the interior vertices $\mathbf{x}_I = (x_{k+1}, \dots, x_n)^T$ and $\mathbf{y}_I = (y_{k+1}, \dots, y_n)^T$ have to satisfy the equilibrium condition (1) for the stress ω . In particular, the equations $\bar{L}\mathbf{x}_I + L_{IB}\mathbf{x}_B = \mathbf{0}$ and

$\bar{L}\mathbf{y}_I + L_{IB}\mathbf{y}_B = \mathbf{0}$ have to hold. Thus, we can express the interior coordinates as

$$\begin{aligned}\mathbf{x}_I &= -\bar{L}^{-1}L_{IB}\mathbf{x}_B, \\ \mathbf{y}_I &= -\bar{L}^{-1}L_{IB}\mathbf{y}_B.\end{aligned}\tag{6}$$

For non-zero weights ω the matrix L_{II} is irreducible (that is, the underlying graph is connected, see Lemma 3.2) and diagonally dominant. As a consequence L_{II} is invertible and (6) has a unique solution [15, page 363].

The barycentric embedding assures that the interior vertices are in equilibrium. However, to make $G(\mathbf{p})$ liftable we have to guarantee the equilibrium also for the vertices on f_0 . We define the vectors $F := \mathbf{F}_1, \dots, \mathbf{F}_k$ as the non-resolving “forces”, which arise at the boundary vertices and cannot be canceled by the interior stresses:

$$\forall i \in B \quad \sum_{(i,j) \in E} \omega_{ij}(\mathbf{p}_i - \mathbf{p}_j) =: \mathbf{F}_i.\tag{7}$$

Our goal is to define the yet unassigned stresses on the boundary edges such that they cancel the forces in F . However, this is not always possible, depending on the shape of the outer face. In order to pick a good embedding of f_0 , we have to know how changing the coordinates of the outer face changes the forces in F . The following lemma helps to express this dependence.

Lemma 3.1 (Substitution Lemma). *There are weights $\tilde{\omega}_{ij} = \tilde{\omega}_{ji}$, for $i, j \in B$, independent of the location of the boundary vertices, such that*

$$\mathbf{F}_i = \sum_{j \in B: j \neq i} \tilde{\omega}_{ij}(\mathbf{p}_i - \mathbf{p}_j).$$

The weights $\tilde{\omega}_{ij}$ are the off-diagonal entries of $L_{BI}\bar{L}^{-1}L_{IB} - L_{BB}$. If ω is integral, each $\tilde{\omega}$ is a multiple of $1/\det \bar{L}$.

Proof. Let \mathbf{F}_x denote the vector $(F_1^x, \dots, F_k^x)^T$, where F_i^x is the x -component of the vector \mathbf{F}_i . We rephrase (7) as $\mathbf{F}_x = L_{BB}\mathbf{x}_B + L_{BI}\mathbf{x}_I$. With help of (6) we eliminate \mathbf{x}_I and obtain

$$\mathbf{F}_x = L_{BB}\mathbf{x}_B - L_{BI}\bar{L}^{-1}L_{IB}\mathbf{x}_B =: \tilde{L}\mathbf{x}_B.$$

(The matrix $\tilde{L} = L_{BB} - L_{BI}\bar{L}^{-1}L_{IB}$ is the Schur complement of \bar{L} in L .) For the y -coordinates, we obtain a similar formula with the same matrix \tilde{L} . We define $\tilde{\omega}_{ij}$ as the off-diagonal entries $-\tilde{l}_{ij}$ of \tilde{L} . Since $L_{BI} = (L_{IB})^T$, the matrix \tilde{L} is symmetric and therefore $\tilde{\omega}_{ij} = \tilde{\omega}_{ji}$ holds.

To show that the expression $\mathbf{F}_x = \tilde{L}\mathbf{x}_B$ has the form stated in the lemma we have to check that all row sums in \tilde{L} equal 0. Let $\mathbf{1}$ denote the vector where all entries are 1, equivalently $\mathbf{0}$ denotes the vector that contains only zeros as entries. Since each of the last $n - k$ rows of L sums up to 0 we have $\bar{L}\mathbf{1} + L_{IB}\mathbf{1} = \mathbf{0}$; and hence $-\bar{L}^{-1}L_{IB}\mathbf{1} = \mathbf{1}$. Plugging this expression into $\tilde{L}\mathbf{1} = L_{BB}\mathbf{1} - L_{BI}\bar{L}^{-1}L_{IB}\mathbf{1}$ gives us $\tilde{L}\mathbf{1} = L_{BB}\mathbf{1} + L_{BI}\mathbf{1}$, which equals $\mathbf{0}$. The matrix \tilde{L} can be written as a rational expression whose denominator is the determinant of \bar{L} , and thus the weights $\tilde{\omega}$ are multiples of $1/\det \bar{L}$. \square

In linear algebra terms, the lemma can be rephrased as saying that the Schur complement of a submatrix of a weighted Laplacian, if it exists, has again the form of a weighted Laplacian.

The proof assumes that \bar{L} is invertible. This is the case whenever the graph G has no connected component that is a subset of I . If such components exist, they can simply be omitted, since they are completely disconnected from B and hence have no effect on the forces in F . Hence, the lemma holds for arbitrary graphs, without any connectivity assumptions.

Example. For the example of Figure 1, we obtain the following substitution stresses.

$$-\tilde{L} = \begin{pmatrix} -\tilde{\omega}_{12} - \tilde{\omega}_{13} & \tilde{\omega}_{12} & \tilde{\omega}_{13} \\ \tilde{\omega}_{12} & -\tilde{\omega}_{12} - \tilde{\omega}_{23} & \tilde{\omega}_{23} \\ \tilde{\omega}_{13} & \tilde{\omega}_{23} & -\tilde{\omega}_{13} - \tilde{\omega}_{23} \end{pmatrix} = \begin{pmatrix} -96/95 & 3/5 & 39/95 \\ 3/5 & -6/5 & 3/5 \\ 39/95 & 3/5 & -96/95 \end{pmatrix}$$

We emphasize that the $\tilde{\omega}$ values are independent of the location of \mathbf{x}_B and \mathbf{y}_B : they only depend on the combinatorial structure of G . In other words, the stresses $\tilde{\omega}_{ij}$ contain all the necessary information about the combinatorial structure of G . Thus, we have a compact description (of size $\binom{k}{2}$) of the structure of G that is responsible for the forces in F . We call the stresses $\tilde{\omega}$ *substitution stresses* to emphasize that they are used as a substitution for the combinatorial structure of G .

For the later analysis of the grid size it is necessary to bound the size of the substitution stresses. We first state a technical lemma.

Lemma 3.2. *Removing all vertices and edges of a face f_0 from a 3-connected planar graph G leaves a connected graph.*

Proof. After realizing G as a polytope, the claim becomes a special case of the well-known statement that a graph of a polytope in any dimension remains connected if the vertices of some face are removed. This statement can be proved by defining a linear objective function that realizes the minimum entirely on the removed vertices. Every remaining vertex is connected to the maximum vertex by a monotone increasing path. The objective function can be perturbed such that there is a unique maximum. \square

Lemma 3.3. 1. *Let ω be a stress that is positive on every interior edge. Any induced substitution stress $\tilde{\omega}_{ij}$ is positive.*

2. *Let ω be the stress that is 1 on every interior edge. Any induced substitution stress $\tilde{\omega}_{ij}$ is smaller than $n - k$.*

Proof. The substitution stresses are independent of the location of f_0 . Therefore, we can choose the positions for the boundary vertices freely. We place vertex v_i at position $(0, 0)^T$ and all other boundary vertices at $(1, 0)^T$. All vertices lie on the segment between $(0, 0)^T$ and $(1, 0)^T$, which is the convex hull of the boundary vertices.

We now show that all interior vertices lie in the interior of this segment. If an interior vertex lies at $(1, 0)^T$ then all its neighbors have to lie at $(1, 0)^T$ as well. Otherwise the vertex cannot be in equilibrium. But since due to Lemma 3.2 all interior vertices are connected by interior edges this would imply that all interior vertices must lie at $(1, 0)^T$. This is a contradiction, since v_i is also the neighbor of an interior vertex. By the same arguments one can show that no interior vertex can lie at $(0, 0)^T$. Therefore, all interior vertices have a positive x -coordinate strictly smaller than 1.

In our special embedding the force \mathbf{F}_j ($j \neq i$) can be expressed as $\mathbf{F}_j = (\tilde{\omega}_{ij}, 0)^T$. By (7) we have $\tilde{\omega}_{ij} = \sum_{k \in I} \omega_{jk}(x_j - x_k)$. Due to the results of the previous paragraph, this sum consists of at most $|I|$ summands, which are positive, and in the case $\omega \equiv 1$ smaller than 1. Both statements of the lemma follow. \square

We are now ready to introduce the embedding algorithm. As a first step we construct a 2d embedding in equilibrium with respect to a stress ω with $\omega \equiv 1$ on the interior edges. In order to get equilibrium on the boundary vertices as well, we have to choose their locations and the stresses on the boundary edges appropriately. This leads to a non-linear system in the $2k$ unknowns \mathbf{x}_B , and \mathbf{y}_B and the k unknown boundary stresses $\omega_{12}, \omega_{23}, \dots, \omega_{k1}$. Let L_0 be the Laplacian of the graph that consists of the outer face f_0 only, with unknown stresses $\omega_{12}, \omega_{23}, \dots, \omega_{k1}$ for the boundary edges. The $2k$ equations of the system are given by

$$L_0 \mathbf{x}_B + \tilde{L} \mathbf{x}_B = \mathbf{0}, \quad L_0 \mathbf{y}_B + \tilde{L} \mathbf{y}_B = \mathbf{0}. \quad (8)$$

Since these equations are dependent, the system is under-constrained. To solve it, we fix as many boundary coordinates as necessary to obtain a unique solution. We also have to ensure that the solution defines a *convex* face. We continue with a case distinction on k .

Case 1: G contains a triangular face

The triangular case is easy: we can position the boundary vertices at any convenient position (see for example [14]). We choose:

$$\mathbf{p}_1 = \begin{pmatrix} 0 \\ 0 \end{pmatrix}, \mathbf{p}_2 = \begin{pmatrix} 1 \\ 0 \end{pmatrix}, \mathbf{p}_3 = \begin{pmatrix} 0 \\ 1 \end{pmatrix}. \quad (9)$$

Lemma 3.4. *If G contains a triangle and we place the boundary vertices as stated in (9) then the boundary forces can be resolved.*

Proof. We embed G as barycentric embedding and calculate the substitution stresses. After setting $\omega_{12} = -\tilde{\omega}_{12}, \omega_{23} = -\tilde{\omega}_{23}, \omega_{13} = -\tilde{\omega}_{13}$ all points are in equilibrium. \square

Case 2: G contains a quadrilateral but no triangular face

If f_0 is a quadrilateral we have to fix some coordinates of the boundary vertices such that it is possible to cancel the forces in F . We used computer algebra software to experiment with various possibilities to constrain the coordinates and solve the non-linear system (8). A unique solution can be obtained by setting

$$\mathbf{p}_1 = \begin{pmatrix} 0 \\ 0 \end{pmatrix}, \mathbf{p}_2 = \begin{pmatrix} 1 \\ 0 \end{pmatrix}, \mathbf{p}_3 = \begin{pmatrix} 2 \\ y_3 \end{pmatrix}, \mathbf{p}_4 = \begin{pmatrix} 0 \\ 1 \end{pmatrix}, \quad (10)$$

with

$$y_3 = \frac{\tilde{\omega}_{24}}{2\tilde{\omega}_{13} - \tilde{\omega}_{24}}. \quad (11)$$

The solution of the equation system (8) provides also the stresses on the boundary edges. These stresses are not necessary for our further computations; we mention them here for completeness only.

$$\begin{aligned} \omega_{12} &= -2\tilde{\omega}_{13} - \tilde{\omega}_{12}, \\ \omega_{23} &= \tilde{\omega}_{24} - 2\tilde{\omega}_{13} - \tilde{\omega}_{23}, \\ \omega_{34} &= -\frac{\tilde{\omega}_{24}}{2} - \tilde{\omega}_{34}, \\ \omega_{14} &= \frac{\tilde{\omega}_{24}\tilde{\omega}_{13}}{\tilde{\omega}_{24} - 2\tilde{\omega}_{13}} - \tilde{\omega}_{14}. \end{aligned} \quad (12)$$

We assume that $\tilde{\omega}_{13} \geq \tilde{\omega}_{24}$. (Otherwise we cyclically relabel the vertices on f_0 .) Since $\omega \equiv 1$ on the interior edges the substitution stresses are positive by Lemma 3.3. Under this assumption we can deduce that $0 < y_3 \leq 1$. Hence, f_0 forms a *convex* face.

Note that the substitution stresses $\tilde{\omega}_{ij}$ between adjacent vertices (on the boundary) are irrelevant. The forces resulting by the boundary stresses $\tilde{\omega}_{ij}$ can be directly canceled by the corresponding stresses ω_{ij} . This can also be observed by looking at the solution of the corresponding equation system: Boundary stresses do not appear in the solution for y_3 . (Furthermore the sum $\tilde{\omega}_{ij} + \omega_{ij}$ for boundary edges (i, j) does not depend on any other boundary stress either.)

Lemma 3.5. *If G contains a quadrilateral and we place the boundary vertices as stated in (10) and (11), then f_0 forms a convex quadrilateral and the boundary stresses (12) cancel the forces F . \square*

Case 3: G contains no triangular and no quadrilateral face

The case if the smallest face of G is a pentagon is more complicated. We have $\binom{5}{2} = 10$ substitution stresses $\tilde{\omega}_{ij}$, but the adjacent ones do not count (by the same reasons given in the previous case). So we are left with five “diagonal” substitution stresses $\tilde{\omega}_{13}, \tilde{\omega}_{14}, \tilde{\omega}_{24}, \tilde{\omega}_{25}$, and $\tilde{\omega}_{35}$.

Like in the previous cases we determine a unique solution of the equation system by fixing some of the coordinates of the outer face. However, we have to make more effort to guarantee the convexity of f_0 . We first observe:

Lemma 3.6. *We can relabel the boundary points for any stress $(\tilde{\omega}_{ij})_{1 \leq i, j \leq 5}$ such that*

$$\tilde{\omega}_{35} \geq \tilde{\omega}_{24} \quad \text{and} \quad \tilde{\omega}_{25} \geq \tilde{\omega}_{13}.$$

Proof. Without loss of generality we assume that the largest stress on an interior edge is $\tilde{\omega}_{35}$. If $\tilde{\omega}_{25} \geq \tilde{\omega}_{13}$ we are done. Otherwise we relabel the vertices by exchanging $\mathbf{p}_3 \leftrightarrow \mathbf{p}_5$ and $\mathbf{p}_1 \leftrightarrow \mathbf{p}_2$. \square

For the rest of this section we label the vertices such that Lemma 3.6 holds. The way we embed f_0 depends on the substitution stresses $\tilde{\omega}_{ij}$.

Case 3A:

We assume that

$$\tilde{\omega}_{35}\tilde{\omega}_{14} + \tilde{\omega}_{14}\tilde{\omega}_{25} + \tilde{\omega}_{25}\tilde{\omega}_{24} + \tilde{\omega}_{13}\tilde{\omega}_{35} > \tilde{\omega}_{35}\tilde{\omega}_{25}. \quad (13)$$

In this case we assign

$$\mathbf{p}_1 = \begin{pmatrix} 0 \\ 0 \end{pmatrix}, \mathbf{p}_2 = \begin{pmatrix} 1 \\ 0 \end{pmatrix}, \mathbf{p}_3 = \begin{pmatrix} 1 \\ 1 \end{pmatrix}, \mathbf{p}_4 = \begin{pmatrix} 0 \\ 1 \end{pmatrix}, \mathbf{p}_5 = \begin{pmatrix} x_5 \\ y_5 \end{pmatrix}.$$

Figure 2(a) illustrates the location of the points. Together with the equations of (8) we obtain as

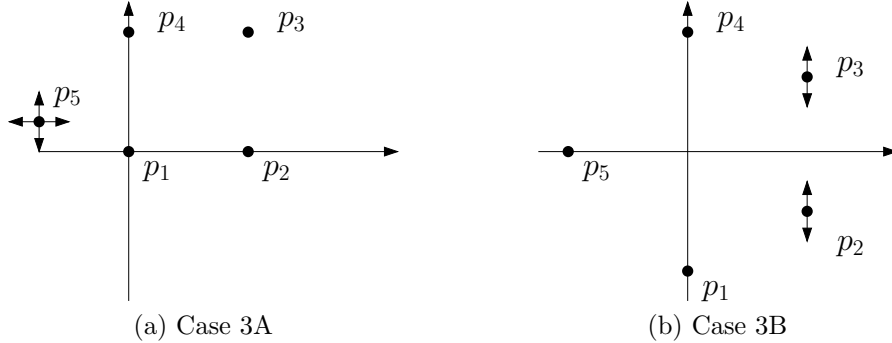


Figure 2: Placement of the boundary vertices.

solution for \mathbf{p}_5 :

$$x_5 = \frac{(\tilde{\omega}_{13} - \tilde{\omega}_{25} - \tilde{\omega}_{24})(\tilde{\omega}_{35} + \tilde{\omega}_{13} - \tilde{\omega}_{24})}{\tilde{\omega}_{35}\tilde{\omega}_{14} + \tilde{\omega}_{14}\tilde{\omega}_{25} + \tilde{\omega}_{25}\tilde{\omega}_{24} + \tilde{\omega}_{13}\tilde{\omega}_{35} - \tilde{\omega}_{35}\tilde{\omega}_{25}},$$

$$y_5 = \frac{\tilde{\omega}_{35} + \tilde{\omega}_{13} - \tilde{\omega}_{24}}{\tilde{\omega}_{35} + \tilde{\omega}_{25}}.$$

The boundary stresses ω_{ij} are complicated expressions that are not necessary for further compu-

tations. We list them here for completeness only.

$$\begin{aligned}
\omega_{12} &= \frac{\tilde{\omega}_{13}(\tilde{\omega}_{25}^2 + \tilde{\omega}_{24}\tilde{\omega}_{35} + 2\tilde{\omega}_{24}\tilde{\omega}_{25} - \tilde{\omega}_{13}\tilde{\omega}_{25}) + \tilde{\omega}_{14}(\tilde{\omega}_{25}^2 + \tilde{\omega}_{25}\tilde{\omega}_{35} + \tilde{\omega}_{24}\tilde{\omega}_{25} + \tilde{\omega}_{35}\tilde{\omega}_{24})}{\tilde{\omega}_{35}\tilde{\omega}_{25} - \tilde{\omega}_{14}\tilde{\omega}_{25} - \tilde{\omega}_{25}\tilde{\omega}_{24} - \tilde{\omega}_{13}\tilde{\omega}_{35} - \tilde{\omega}_{35}\tilde{\omega}_{14}} - \tilde{\omega}_{12}, \\
\omega_{34} &= \frac{\tilde{\omega}_{14}(\tilde{\omega}_{35}^2 + \tilde{\omega}_{35}\tilde{\omega}_{13} + \tilde{\omega}_{25}\tilde{\omega}_{35} + \tilde{\omega}_{13}\tilde{\omega}_{25}) + \tilde{\omega}_{24}(\tilde{\omega}_{35}^2 + \tilde{\omega}_{13}\tilde{\omega}_{25} + 2\tilde{\omega}_{13}\tilde{\omega}_{35} - \tilde{\omega}_{35}\tilde{\omega}_{24})}{\tilde{\omega}_{35}\tilde{\omega}_{25} - \tilde{\omega}_{14}\tilde{\omega}_{25} - \tilde{\omega}_{25}\tilde{\omega}_{24} - \tilde{\omega}_{13}\tilde{\omega}_{35} - \tilde{\omega}_{35}\tilde{\omega}_{14}} - \tilde{\omega}_{34}, \\
\omega_{23} &= \frac{\tilde{\omega}_{13}\tilde{\omega}_{25} + \tilde{\omega}_{25}\tilde{\omega}_{35} + \tilde{\omega}_{24}\tilde{\omega}_{25}}{-\tilde{\omega}_{25} - \tilde{\omega}_{35}} - \tilde{\omega}_{23}, \\
\omega_{45} &= \frac{\tilde{\omega}_{24}\tilde{\omega}_{25} + \tilde{\omega}_{25}\tilde{\omega}_{14} + \tilde{\omega}_{14}\tilde{\omega}_{35} + \tilde{\omega}_{24}\tilde{\omega}_{35}}{\tilde{\omega}_{13} - \tilde{\omega}_{24} - \tilde{\omega}_{25}} - \tilde{\omega}_{45}, \\
\omega_{15} &= \frac{\tilde{\omega}_{13}\tilde{\omega}_{25} + \tilde{\omega}_{35}\tilde{\omega}_{13} + \tilde{\omega}_{14}\tilde{\omega}_{25} + \tilde{\omega}_{14}\tilde{\omega}_{35}}{\tilde{\omega}_{24} - \tilde{\omega}_{35} - \tilde{\omega}_{13}} - \tilde{\omega}_{15}.
\end{aligned}$$

We have to check that f_0 forms a convex polygon. Clearly, $y_5 > 0$, since the $\tilde{\omega}_{ij}$'s are greater than zero and $\tilde{\omega}_{35} \geq \tilde{\omega}_{24}$. Moreover $y_5 < 1$, because $\tilde{\omega}_{25} \geq \tilde{\omega}_{13}$. The numerator of x_5 is negative and due to (13) the denominator of x_5 is positive. Therefore, $x_5 < 0$ and f_0 forms a convex polygon.

Case 3B:

We assume the opposite of (13), namely

$$\tilde{\omega}_{35}\tilde{\omega}_{14} + \tilde{\omega}_{14}\tilde{\omega}_{25} + \tilde{\omega}_{25}\tilde{\omega}_{24} + \tilde{\omega}_{13}\tilde{\omega}_{35} \leq \tilde{\omega}_{35}\tilde{\omega}_{25}. \quad (14)$$

The coordinates for the boundary vertices are chosen as

$$\mathbf{p}_1 = \begin{pmatrix} 0 \\ -1 \end{pmatrix}, \mathbf{p}_2 = \begin{pmatrix} 1 \\ y_2 \end{pmatrix}, \mathbf{p}_3 = \begin{pmatrix} 1 \\ y_3 \end{pmatrix}, \mathbf{p}_4 = \begin{pmatrix} 0 \\ 1 \end{pmatrix}, \mathbf{p}_5 = \begin{pmatrix} -1 \\ 0 \end{pmatrix}.$$

See Figure 2(b) for an illustration. This leads to the solution

$$\begin{aligned}
y_2 &= -2 \cdot \frac{\tilde{\omega}_{24}\tilde{\omega}_{13} + \tilde{\omega}_{24}\tilde{\omega}_{35} + \tilde{\omega}_{25}\tilde{\omega}_{13} + 2\tilde{\omega}_{25}\tilde{\omega}_{35} - \tilde{\omega}_{13}^2 - 2\tilde{\omega}_{13}\tilde{\omega}_{35} - \tilde{\omega}_{35}\tilde{\omega}_{14}}{\tilde{\omega}_{24}\tilde{\omega}_{35} + \tilde{\omega}_{25}\tilde{\omega}_{13} + 2\tilde{\omega}_{25}\tilde{\omega}_{35}}, \\
y_3 &= 2 \cdot \frac{\tilde{\omega}_{24}\tilde{\omega}_{13} + \tilde{\omega}_{24}\tilde{\omega}_{35} + \tilde{\omega}_{25}\tilde{\omega}_{13} + 2\tilde{\omega}_{25}\tilde{\omega}_{35} - \tilde{\omega}_{24}^2 - 2\tilde{\omega}_{24}\tilde{\omega}_{25} - \tilde{\omega}_{14}\tilde{\omega}_{25}}{\tilde{\omega}_{24}\tilde{\omega}_{35} + \tilde{\omega}_{25}\tilde{\omega}_{13} + 2\tilde{\omega}_{25}\tilde{\omega}_{35}}.
\end{aligned}$$

The boundary stresses ω_{ij} are once more not necessary for further computations and listed for completeness only.

$$\begin{aligned}
\omega_{12} &= -\tilde{\omega}_{24} - 2\tilde{\omega}_{25} - \tilde{\omega}_{12}, \\
\omega_{23} &= \frac{-\tilde{\omega}_{25}(\tilde{\omega}_{13}^2 + 2\tilde{\omega}_{13}\tilde{\omega}_{35} + 2\tilde{\omega}_{24}\tilde{\omega}_{35}) - \tilde{\omega}_{35}(\tilde{\omega}_{24}^2 + \tilde{\omega}_{25}\tilde{\omega}_{14})}{2\tilde{\omega}_{35}(\tilde{\omega}_{24} + \tilde{\omega}_{25} - \tilde{\omega}_{13} - \frac{1}{2}\tilde{\omega}_{14}) + 2\tilde{\omega}_{25}(\tilde{\omega}_{13} + \tilde{\omega}_{35} - \tilde{\omega}_{24} - \frac{1}{2}\tilde{\omega}_{14}) - (\tilde{\omega}_{13} - \tilde{\omega}_{24})^2} - \tilde{\omega}_{23}, \\
\omega_{34} &= -\tilde{\omega}_{14} - 2\tilde{\omega}_{15} - \tilde{\omega}_{34}, \\
\omega_{45} &= \tilde{\omega}_{24} - 2\tilde{\omega}_{35} - \tilde{\omega}_{13} - \tilde{\omega}_{45}, \\
\omega_{15} &= \tilde{\omega}_{13} - 2\tilde{\omega}_{25} - \tilde{\omega}_{24} - \tilde{\omega}_{15}.
\end{aligned}$$

The outer face is convex if $-2 < y_2 < y_3 < 2$. The inequalities $-2 < y_2$ and $y_3 < 2$ are equivalent to

$$\begin{aligned}
-\tilde{\omega}_{13}^2 - \tilde{\omega}_{35}\tilde{\omega}_{14} + \tilde{\omega}_{13}(\tilde{\omega}_{24} - 2\tilde{\omega}_{35}) &< 0 \text{ and} \\
-\tilde{\omega}_{24}^2 - \tilde{\omega}_{14}\tilde{\omega}_{25} + \tilde{\omega}_{24}(\tilde{\omega}_{13} - 2\tilde{\omega}_{25}) &< 0.
\end{aligned}$$

Both inequalities hold, because we add only negative summands on the left side. It remains to check if $y_2 - y_3 < 0$. First we get rid of the denominator and bring all negative summands on the right side. This leads to the equivalent inequality

$$\begin{aligned} \tilde{\omega}_{13}^2 + \tilde{\omega}_{24}^2 + 2\tilde{\omega}_{13}\tilde{\omega}_{35} + 2\tilde{\omega}_{24}\tilde{\omega}_{25} + \tilde{\omega}_{25}\tilde{\omega}_{14} + \tilde{\omega}_{35}\tilde{\omega}_{14} < \\ 2\tilde{\omega}_{24}\tilde{\omega}_{35} + 2\tilde{\omega}_{25}\tilde{\omega}_{13} + 4\tilde{\omega}_{25}\tilde{\omega}_{35} + 2\tilde{\omega}_{24}\tilde{\omega}_{13}. \end{aligned} \quad (15)$$

We observe that $\tilde{\omega}_{13}^2 \leq \tilde{\omega}_{25}\tilde{\omega}_{13}$ and $\tilde{\omega}_{24}^2 \leq \tilde{\omega}_{24}\tilde{\omega}_{35}$. Because of the assumption (14) we have $4\tilde{\omega}_{35}\tilde{\omega}_{25} > 2\tilde{\omega}_{13}\tilde{\omega}_{35} + 2\tilde{\omega}_{24}\tilde{\omega}_{25} + \tilde{\omega}_{25}\tilde{\omega}_{14} + \tilde{\omega}_{35}\tilde{\omega}_{14}$. Therefore, the right side of (15) is greater than its left side, which shows that $y_2 < y_3$ and f_0 forms a convex pentagon. This completes the case distinction and we conclude with the following lemma.

Lemma 3.7. *If we place the boundary vertices as discussed above, then the outer face will be embedded as a convex pentagon and the computed boundary stresses cancel the forces in F .* \square

We have defined four different ways to embed G . The selected embedding depends on the combinatorial structure G . If G contains a triangular face we say it is of *type 3*. If it contains a quadrilateral but no triangular face G is of *type 4*. Otherwise the embedding depends on the substitution stresses induced by the combinatorial structure of G . If (13) holds (Case 3A) G is of *type 5A*, otherwise (Case 3B) we say G is of *type 5B*.

3.2 Lifting the Plane Embedding and Scaling to Integrality

We continue with lifting the plane embedding of G to \mathbb{R}^3 . With help of the observations made in Section 2 the incremental computation of the 3d embedding is straightforward. It suffices to compute for every face f_i the corresponding plane H_i .

Since the embedding of f_0 is convex, the boundary stresses must necessarily be negative, since otherwise the boundary vertices could not be in equilibrium with all interior stresses being positive. Thus we do not need to explicitly check the sign of the boundary stresses. The sign pattern of the stress implies that the lifting of the plane embedding gives a convex polytope (see Proposition 1).

As described in Section 2, we begin the lifting by fixing the plane H_1 for some interior face f_1 as the x - y -plane. We set $\mathbf{a}_1 = (0, 0)^T$, $d_1 = 0$, and compute the remaining planes face by face using equations (4) and (5). It is not necessary to compute the parameters of H_0 since we can determine the heights of $\mathbf{p}_1, \dots, \mathbf{p}_k$ by some plane H_i of an interior face. Hence, the lifting can be computed using only stresses on interior edges. This simplifies the later analysis because all interior stresses are 1, whereas the boundary stresses are complicated expressions.

It can be observed that the computed lifting has rational coordinates. This is true because the barycentric embedding gives rational coordinates and the lifting process is based on multiplication and addition of the 2d coordinates. Hence, the z -coordinates are also rational. We analyze the common denominator of the coordinates to obtain scaling factors for the integral embedding. We use different scaling factors S_x for the x -coordinates and S_y for the y -coordinates.

As a consequence of Lemma 2.1 it is sufficient to scale to integer x and y -coordinates. Furthermore we observe:

Lemma 3.8. *If the boundary points are integral, the barycentric embedding yields coordinates that are multiples of $1/\det \bar{L}$.*

Proof. The interior plane coordinates are a result of equation (6). By Cramer's rule every coordinate can be expressed as

$$x_i = \det \bar{L}^{(i)} / \det \bar{L},$$

where $\det \bar{L}^{(i)}$ is obtained from \bar{L} by replacing the i -th column of \bar{L} by $L_{IB}\mathbf{x}_B$. Since $\det \bar{L}^{(i)}$ is integral, $\det \bar{L}$ is the denominator of x_i . The same holds for y_i . \square

Our first goal is to scale the plane embedding such that the boundary vertices get integer coordinates. Let S_x^B be the integral scaling factor that gives integer *boundary* x -coordinates and S_y^B be the integral scaling factor that gives integer *boundary* y -coordinates. Due to Lemma 3.8 the scaling factors $S_x := S_x^B \det \bar{L}$ and $S_y := S_y^B \det \bar{L}$ make all vertices integral. Since we choose integral scaling factors S_x^B and S_y^B no integer coordinate is scaled to a non-integer.

Let us now compute the factors that are necessary to scale to integer boundary coordinates. Clearly the scaling factors depend on the type of G . If G is of type 3 then we need not scale, since all boundary coordinates are either 0 or 1. If G is of type 4 we have to scale the y -coordinates only (see 11). We multiply y_3 with $S_y^B := (2\tilde{\omega}_{13} - \tilde{\omega}_{24}) \det \bar{L}$, which gives $S_y^B y_3 = \tilde{\omega}_{24} \det \bar{L}$, which due to the Substitution Lemma is an integer.

If G is of type 5A we have to scale such that x_5 and y_5 become integral. We pick

$$\begin{aligned} S_x^B &= (\tilde{\omega}_{35}\tilde{\omega}_{14} + \tilde{\omega}_{14}\tilde{\omega}_{25} + \tilde{\omega}_{25}\tilde{\omega}_{24} + \tilde{\omega}_{13}\tilde{\omega}_{35} - \tilde{\omega}_{35}\tilde{\omega}_{25})(\det \bar{L})^2, \\ S_y^B &= (\tilde{\omega}_{35} + \tilde{\omega}_{25}) \det \bar{L}. \end{aligned}$$

It can be easily checked that these factors as well as $S_x^B x_5$ and $S_y^B y_5$ are integral.

When G is of type 5B, the only non-integer boundary coordinates are y_2 and y_3 , we need to scale in y -direction only. We choose

$$S_y^B = (\tilde{\omega}_{24}\tilde{\omega}_{35} + \tilde{\omega}_{25}\tilde{\omega}_{13} + 2\tilde{\omega}_{25}\tilde{\omega}_{35})(\det \bar{L})^2.$$

Again, due to the Substitution Lemma, S_y^B , $S_y^B y_2$, and $S_y^B y_3$ are all integral.

For every type of G there is a pair of scaling factors S_x, S_y , such that the scaled boundary points are integral. Table 1 summarizes the discussion and lists the final scaling factors depending on the type of G .

type of G	scaling factors
3	$S_x = S_y = \det \bar{L}$
4	$S_x = \det \bar{L}$ $S_y = (2\tilde{\omega}_{13} - \tilde{\omega}_{24})(\det \bar{L})^2$
5A	$S_x = (\tilde{\omega}_{35}\tilde{\omega}_{14} + \tilde{\omega}_{14}\tilde{\omega}_{25} + \tilde{\omega}_{25}\tilde{\omega}_{24} + \tilde{\omega}_{13}\tilde{\omega}_{35} - \tilde{\omega}_{35}\tilde{\omega}_{25})(\det \bar{L})^3$ $S_y = (\tilde{\omega}_{35} + \tilde{\omega}_{25})(\det \bar{L})^2$
5B	$S_x = \det \bar{L}$ $S_y = (\tilde{\omega}_{24}\tilde{\omega}_{35} + \tilde{\omega}_{25}\tilde{\omega}_{13} + 2\tilde{\omega}_{25}\tilde{\omega}_{35})(\det \bar{L})^3$

Table 1: The scaling factors S_x and S_y for the different types of G .

3.3 Analysis of the Grid Size

To bound the size of the coordinates of the integer embedding it is crucial to obtain a good bound for $\det \bar{L}$. Recall that we assume unit stresses $\omega \equiv 1$ on the interior edges, throughout. There exists a connection between the number of spanning trees in G and $\det \bar{L}$. Let us first define:

Definition 2. Let \mathcal{B} be a subset of vertices of G . A subgraph of G is called spanning \mathcal{B} -forest if

- it consists of $|\mathcal{B}|$ vertex disjoint trees covering all vertices of G ,
- each tree contains a unique vertex from \mathcal{B} .

In the following we use the set of boundary vertices for \mathcal{B} . Let $\mathcal{F}_B(G)$ denote the number of spanning B -forests of G and $\mathcal{T}(G)$ the number of spanning trees of G . A generalization of the Matrix-Tree Theorem [16] (see also [21]) states that the number of spanning B -forests of G is $\det \bar{L}$. In our case, we can directly bound $\mathcal{F}_B(G)$ by $\mathcal{T}(G)$.

Lemma 3.9. *Let G be a planar graph with a distinguished face and let B be the set of vertices of this face. The number of spanning B -forests of G is bounded from above by*

$$\mathcal{F}_B(G) < \mathcal{T}(G).$$

Proof. Every spanning B -forest can be turned into a spanning tree by adding all boundary edges except $(1, 2)$. No two distinct spanning B -forests are associated with the same spanning tree. Therefore, the number of spanning trees exceeds the number of spanning B -forests. Since there is a spanning tree that contains the edge $(1, 2)$ the inequality is strict. \square

It is easy to give an exponential upper bound for $\mathcal{T}(G)$:

Proposition 2 (Ribó Mor [21]). *1. The number of spanning trees in a graph is bounded by the product of all vertex degrees:*

$$\mathcal{T}(G) < \prod_i \deg(v_i).$$

2. For a planar graph, we have $\mathcal{T}(G) < \prod_i \deg(v_i) < 6^n$.

Proof. 1. Consider all directed graphs that are obtained by choosing an outgoing edge in G out of every vertex except v_n . The number of these directed graphs is given by $\prod_{i=1}^{n-1} \deg(v_i)$. By ignoring the edge orientations, one obtains all spanning trees (and many graphs that are not spanning trees). Alternatively, the bound can be proved by applying a variant of Hadamard's inequality for positive semidefinite matrices [37, page 176] to the (positive semidefinite) matrix L' that is obtained by removing from the Laplacian L the row and column corresponding to the vertex v_n :

$$\mathcal{T}(G) = \det \bar{L} \leq \prod_{i=1}^{n-1} l_{ii} = \prod_{i=1}^{n-1} \deg(v_i)$$

2. This follows from the arithmetic-geometric-mean inequality and the fact that $\sum_i \deg(v_i) < 6n$, which is a consequence of Euler's formula. \square

Sharper bounds for $\mathcal{T}(G)$ have been given by Ribó Mor et al. [23], see also [21, 26]. These bounds take into account whether G contains triangular or quadrilateral faces:

$$\begin{aligned} \text{if } G \text{ is of type 3: } & \mathcal{F}_B(G) < \mathcal{T}(G) \leq 5.3^n, \\ \text{if } G \text{ is of type 4: } & \mathcal{F}_B(G) < \mathcal{T}(G) \leq 3.529988^n, \\ \text{if } G \text{ is of type 5A/5B: } & \mathcal{F}_B(G) < \mathcal{T}(G) \leq 2.847263^n. \end{aligned}$$

Since we know upper bounds for the $\tilde{\omega}$ values (by Lemma 3.3) and $\det \bar{L}$ (by the previous discussion) we can bound the size of the integer coordinates of the embedding of G . We start with bounding the x and y -coordinates. Let Δx denote an upper bound for the difference between the largest and the smallest x -coordinate. Δy is defined in the same way for the y -coordinates.

Again we have to discuss the 4 cases separately. If G is of type 3 then clearly $\Delta x = \Delta y = \det \bar{L}$. If G is of type 4 the largest x -coordinate is $2S_x$ and the smallest zero. Thus we have $\Delta x = 2 \det \bar{L}$. The largest y -coordinate is obtained at $y_4 = 1$ (remember $y_3 \leq 1$), therefore $\Delta y = S_y = (2\tilde{\omega}_{13} - \tilde{\omega}_{24})(\det \bar{L})^2$. Let us now assume G is of type 5A. The value of Δx is given by $x_2 - x_5$. Evaluating this expression leads to

$$\Delta x = (\tilde{\omega}_{25}(\tilde{\omega}_{13} + \tilde{\omega}_{14}) + \tilde{\omega}_{35}(\tilde{\omega}_{14} + \tilde{\omega}_{25}) - (\tilde{\omega}_{13} - \tilde{\omega}_{24})^2)(\det \bar{L})^3.$$

type of G	Δx
3	$\det \bar{L}$
4	$2 \det \bar{L}$
5A	$(\tilde{\omega}_{25}(\tilde{\omega}_{13} + \tilde{\omega}_{14}) + \tilde{\omega}_{35}(\tilde{\omega}_{14} + \tilde{\omega}_{25}) - (\tilde{\omega}_{13} - \tilde{\omega}_{24})^2)(\det \bar{L})^3$
5B	$2 \det \bar{L}$

Table 2: The values Δx depending on the type of G .

type of G	Δy
3	$\det \bar{L}$
4	$(2\tilde{\omega}_{13} - \tilde{\omega}_{24})(\det \bar{L})^2$
5A	$(\tilde{\omega}_{35} + \tilde{\omega}_{25})(\det \bar{L})^2$
5B	$4(\tilde{\omega}_{24}\tilde{\omega}_{35} + \tilde{\omega}_{25}\tilde{\omega}_{13} + 2\tilde{\omega}_{25}\tilde{\omega}_{35})(\det \bar{L})^3$

Table 3: The values Δy depending on the type of G .

Since the smallest y -coordinate is zero we have $\Delta y = y_3$, which equals $(\tilde{\omega}_{35} + \tilde{\omega}_{25})(\det \bar{L})^2$. It remains to discuss the case when G is of type 5B. *Before* the scaling the coordinates fulfill $-1 \leq x \leq 1$ and $-2 < y < 2$. Combining these inequalities with the scaling factors yields $\Delta x = 2 \det \bar{L}$ and $\Delta y = 4(\tilde{\omega}_{24}\tilde{\omega}_{35} + \tilde{\omega}_{25}\tilde{\omega}_{13} + 2\tilde{\omega}_{25}\tilde{\omega}_{35})(\det \bar{L})^3$. We sum up the results for Δx and Δy in Table 2 and Table 3. With help of Lemma 3.3 we can eliminate the $\tilde{\omega}$ values that appear in the bounds of Δx and Δy . The resulting upper bounds, which we use in the further analysis, are listed in Table 4.

We finish the analysis of the necessary grid size by calculating the size of the z -coordinates.

Lemma 3.10. *Let $G(\mathbf{p})$ be an integral $2d$ embedding of a graph with n vertices with equilibrium stress ω and let the stress on all interior edges be 1. The difference between two x -coordinates is at most Δx and the difference between two y -coordinates is at most Δy . Then we have an integral lifting with*

$$0 \leq z_i < 2n\Delta x\Delta y$$

for all z -coordinates z_i .

Proof. Due to Lemma 2.1 we know that there exists an integral lifting for the setting described in the lemma. We place an interior face f_1 in the xy -plane and compute the lifting by using the stresses on the interior edges. Notice that all z -coordinates are non-positive in this lifting. Thus it suffices to compute the smallest z -coordinate. The claimed lifting is then obtained by translating the polytope such that the smallest z -coordinate becomes 0.

We choose as face f_1 a face that shares an edge with the outer face f_0 . Furthermore we assume that the boundary point farthest away from the line that contains $f_1 \cap f_0$ is located in the origin

type of G	upper bound for Δx	upper bound for Δy
3	$\det \bar{L}$	$\det \bar{L}$
4	$2 \det \bar{L}$	$2n(\det \bar{L})^2$
5A	$4n^2(\det \bar{L})^3$	$2n(\det \bar{L})^2$
5B	$2 \det \bar{L}$	$16n^2(\det \bar{L})^3$

Table 4: Upper bounds for Δx and Δy depending on the type of G .

(let this point be \mathbf{p}_1). This is no restriction since a translation of the embedding does not interfere with the lifting. The lifted polytope lies below the xy -plane H_1 and above H_0 . We notice that the smallest z -coordinate of H_0 (and hence the smallest z -coordinate of the embedding) is realized at \mathbf{p}_1 .

Let f_k be an interior face that contains \mathbf{p}_1 . The z -coordinate of \mathbf{p}_1 is given as

$$z_1 = \langle \mathbf{a}_k, \mathbf{p}_1 \rangle + d_k = d_k.$$

The variable d_k can be computed with help of equation (5). Let \mathcal{C} be a set of interior edges that are crossed by “walking” from f_1 to f_k . Due to Euler’s formula G has at most $2n - 4$ faces. No face is entered twice and thus every face contributes at most one edge (the edge where the “walk” leaves the face) to the set \mathcal{C} . This implies that \mathcal{C} includes at most $2n - 3$ edges. We ignore the orientation of the edges at this place since it does not matter for bounding d_k . We deduce

$$-d_k \leq \sum_{(i,j) \in \mathcal{C}} |\langle \mathbf{p}_i, \mathbf{p}_j^\perp \rangle| < 2n \max\{ |\langle \mathbf{p}_i, \mathbf{p}_j^\perp \rangle| : 1 \leq i, j \leq n \}.$$

For two points $\mathbf{p}_i, \mathbf{p}_j$ we have

$$\langle \mathbf{p}_i, \mathbf{p}_j^\perp \rangle = x_i y_j - x_j y_i.$$

Thus, $\langle \mathbf{p}_i, \mathbf{p}_j^\perp \rangle$ equals two times the negative area of the triangle spanned by $\mathbf{p}_i, \mathbf{p}_j$, and the origin (which coincides with \mathbf{p}_1). This triangle is contained inside the embedded outer face f_0 and also inside a rectangle with edge lengths Δx and Δy . A rectangle has at least twice the area of an inscribed triangle. To see this, observe that an inscribed triangle with the largest area must have one of the rectangle edges as base and the other as height. Thus $|\langle \mathbf{p}_i, \mathbf{p}_j^\perp \rangle| \leq \Delta x \Delta y$ and the smallest z -coordinate is larger than $-2n \Delta x \Delta y$. \square

By applying Lemma 3.10, we compute the bounds for the z -coordinates, using the values of Δx and Δy listed in Table 4. We conclude with the main theorems.

Theorem 3.1. *Every 3-polytope with n vertices whose graph contains at least a triangle can be realized on an integer grid with*

$$\begin{aligned} 0 &\leq x_i, y_i < 5 \cdot \bar{3}^n, \\ 0 &\leq z_i < 2n \cdot 28 \cdot \bar{4}^n. \end{aligned}$$

Theorem 3.2. *Every 3-polytope with n vertices whose graph contains at least one quadrilateral face can be realized on an integer grid with*

$$\begin{aligned} 0 &\leq x_i < 2 \cdot 3.530^n, \\ 0 &\leq y_i < 2n \cdot 12.461^n, \\ 0 &\leq z_i < 8n^2 \cdot 43.987^n. \end{aligned}$$

For the most general theorem we have to combine the analysis for the cases 5A and 5B. We rotate the embedding if G is of type 5B by exchanging its x and y -coordinates to obtain a better bound. The largest z -coordinate is given by $\max\{16n^4 \cdot 187.128^n, 64n^3 \cdot 65.722^n\} = 16n^4 \cdot 187.128^n$, since $n > 4$ if G contains a pentagon. Thus the largest bound on the z -coordinate arises from case 5A.

Theorem 3.3. *Every 3-polytope with n vertices can be realized on an integer grid with*

$$\begin{aligned} 0 &\leq x_i < 16n^2 \cdot 23.083^n, \\ 0 &\leq y_i < 2n \cdot 8.107^n, \\ 0 &\leq z_i < 16n^4 \cdot 187.128^n. \end{aligned}$$

We can improve the constant factor of the z -coordinate by a more careful analysis. This can be achieved by placing the face f_0 in the xy -plane and then compute the lifting using the interior edges but also one boundary edge. As mentioned before the structure of the stresses on the boundary edges is more complicated. Since the improvement would only be a constant factor we decided to present the easier analysis with help of Lemma 3.10. The more complicated analysis can be found in [22].

We see that exponentially large coordinates suffice to embed G as 3-polytope. The exponential growth of the size of the coordinates is determined by $(\det \bar{L})^5$.

Corollary 3.1. *Every 3-polytope with n vertices can be realized with integer coordinates of size $O(2^{7.55n})$.*

Let us add some remarks on the running time of the embedding algorithm. If we know the substitution stresses the computation of the location of the outer face can be done in constant time. The same is true for the scaling factors. Once we computed the plane embedding, the lifting can be computed face by face, which needs in total $O(n)$ steps. The computation of the substitution stresses and of the interior vertices can be done by solving a linear system. Since its underlying structure is planar, we can use nested dissections based on the planar separator theorem to solve it [17, 18]. This implies that a solution can be computed in $O(M(\sqrt{n}))$ time, where $M(n)$ is the upper bound for multiplying two $n \times n$ matrices. The current record for $M(n)$ is $O(n^{2.325})$ which is due Coppersmith and Winograd [8]. Thus the overall running time is given by $O(n^{1.163})$ arithmetic operations.

4 An Example: the Dodecahedron

The regular dodecahedron is one of the five Platonic solids. It has 20 vertices, 30 edges and 12 faces, which are regular pentagons. Figure 3 shows the graph and a 3-dimensional realization of it. It is the smallest polytope without triangles and quadrilateral faces, and thus we have to apply the more involved cases. Since the dodecahedron is symmetric it makes no difference which face

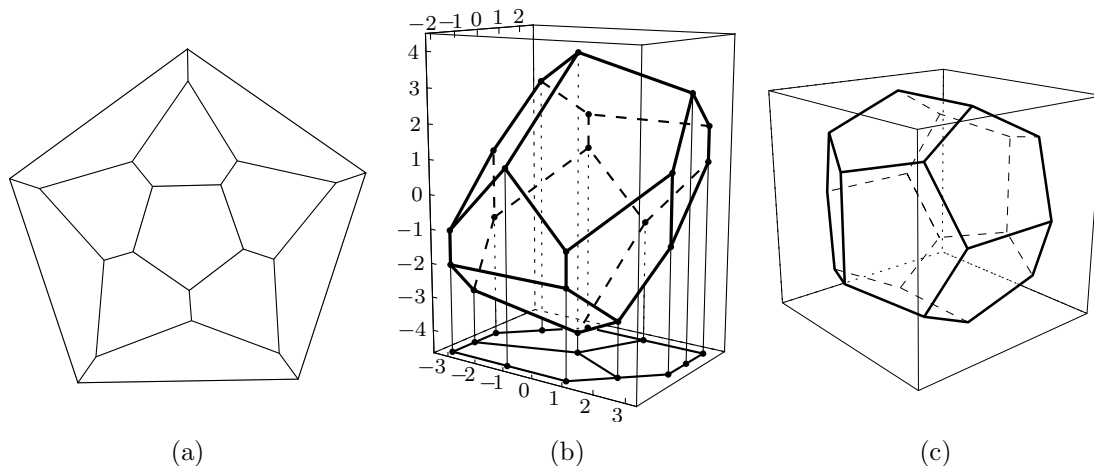


Figure 3: (a) The graph of the dodecahedron and (b,c) two realizations as 3-polytope.

we choose as the outer face. We start the computation with calculating the $\tilde{\omega}$ values. Remember, these values are the off-diagonal entries of the matrix $-(L_{BB} - L_{BI}\bar{L}^{-1}L_{IB})$. We obtain for all the stresses $\tilde{\omega}_{13}, \tilde{\omega}_{14}, \tilde{\omega}_{24}, \tilde{\omega}_{25}$ and $\tilde{\omega}_{35}$ the value $36/449$. The fact that all these stresses have the same value is again due to the symmetry of the dodecahedron. Since the outer face is a 5-gon, G is of

type 5A or 5B. Evaluating (13) shows that the graph is of type 5A. With help of the substitution stresses we compute the coordinates of the boundary vertices. We obtain

$$\mathbf{p}_1 = \begin{pmatrix} 0 \\ 0 \end{pmatrix}, \mathbf{p}_2 = \begin{pmatrix} 1 \\ 0 \end{pmatrix}, \mathbf{p}_3 = \begin{pmatrix} 1 \\ 1 \end{pmatrix}, \mathbf{p}_4 = \begin{pmatrix} 0 \\ 1 \end{pmatrix}, \mathbf{p}_5 = \begin{pmatrix} -1/3 \\ 1/2 \end{pmatrix}.$$

We apply Tutte's method to compute the coordinates of the interior points. The result is depicted in Figure 4. Next, we scale the 2d-embedding as described in Section 3.2. We obtain $\det \bar{L} = 403202$.

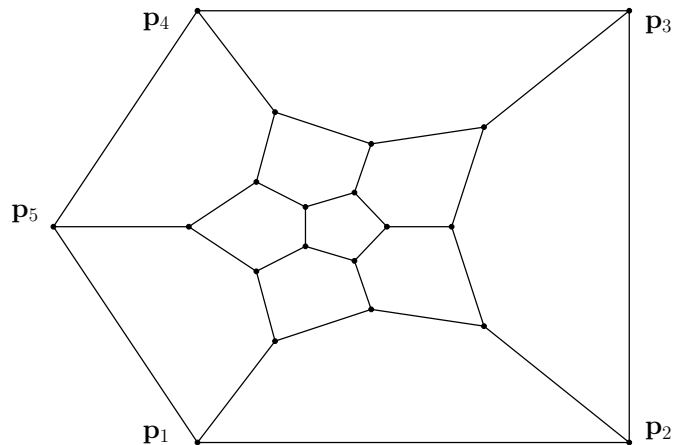


Figure 4: The barycentric (plane) embedding of the dodecahedron.

This yields the scaling factors

$$\bar{S}_x = 1\,264\,158\,727\,403\,904, \quad \bar{S}_y = 26\,069\,428\,512.$$

We continue with the lifting of the plane embedding to \mathbb{R}^3 . The faces are lifted incrementally as described in Section 2. The numeric data of the lifting are listed in [29]. Figure 5 shows the computed embedding. We have scaled down the z -coordinates to obtain an illustrative picture. The highest absolute coordinate is

$$|z_3| = 11\,083\,163\,098\,782\,678\,334\,820\,352 \approx 2^{83.19},$$

which is smaller than the bound 2^{151} from Corollary 3.1.

The computed embedding allows a smaller integer realization. Due to the fact that the greatest common divisor of the x -coordinates is $938\,499\,426\,432 = 449^3 \times 10365$ and the greatest common divisor of the y -coordinates is $29\,030\,544 = 449^2 \times 144$, scaling down by these factors yields a smaller integer embedding. We obtain an integral plane embedding on the grid $[-27, 1347] \times [0, 898]$. The corresponding z -coordinates range between 0 and 406 497. This reduction is due to the fact that all substitution stresses $\tilde{\omega}$ are equal. Thus one might have replaced them by $\tilde{\omega} \equiv 1$ in the subsequent calculations.

A much smaller grid embedding of the dodecahedron was constructed by hand by Francisco Santos. It is centrally symmetric and fits inside a $6 \times 4 \times 8$ box, see Figure 3(b). It is hard to believe that a smaller realization would be possible. Another, more symmetric, realization of the dodecahedron is the pyritohedron (one of the possible crystal shapes of the mineral pyrite), as pointed out to us by Gábor Gévay. It fits in a $12 \times 12 \times 12$ box, see Figure 3(c). It has 8 vertices of the form $(\pm 4, \pm 4, \pm 4)$, plus 12 vertices, which are the 4 vertices of the form $(0, \pm 3, \pm 6)$ and their cyclic rotations of the coordinates. The normals of the 12 faces are the vectors $(0, \pm 2, \pm 1)$ and their cyclic rotations.

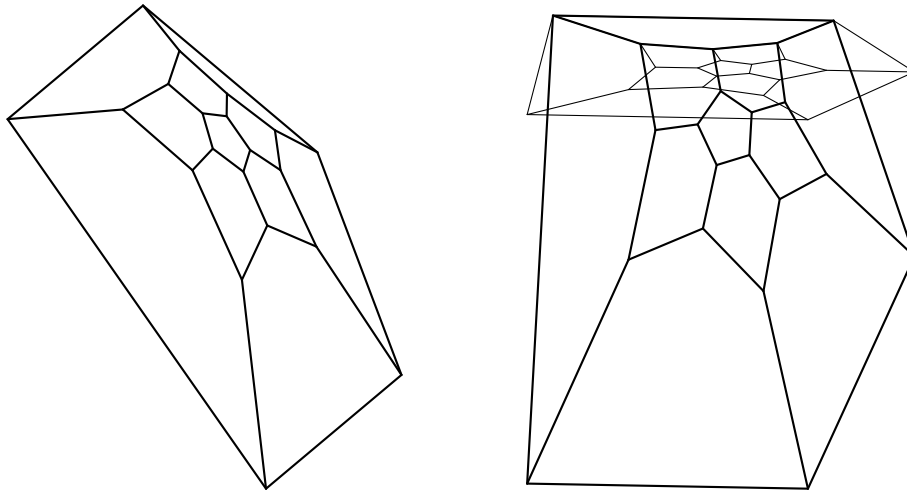


Figure 5: Two views of the dodecahedron embedded with our algorithm, with scaled z -axis. The right picture includes also the equilibrium-stressed plane embedding.

Acknowledgements. We thank a referee for a very thorough reading of the manuscript.

References

- [1] D. M. Acketa and J. D. Žunić. On the maximal number of edges of convex digital polygons included into an $m \times m$ -grid. *J. Comb. Theory Ser. A*, 69(2):358–368, 1995.
- [2] G. E. Andrews. A lower bound for the volume of strictly convex bodies with many boundary lattice points. *Trans. Amer. Math. Soc.*, 99:272–277, 1961.
- [3] I. Bárány and G. Rote. Strictly convex drawings of planar graphs. *Documenta Math.*, 11:369–391, 2006.
- [4] N. Bonichon, S. Felsner, and M. Mosbah. Convex drawings of 3-connected planar graphs. *Algorithmica*, 47:399–420, 2007.
- [5] K. Buchin and A. Schulz. On the number of spanning trees a planar graph can have. In *Proceedings of the 18th Annual European Symposium on Algorithms, (ESA 2010)*, volume to appear, 2010.
- [6] M. Chrobak, M. T. Goodrich, and R. Tamassia. Convex drawings of graphs in two and three dimensions (preliminary version). In *12th Annual Symposium on Computational Geometry*, pages 319–328, 1996.
- [7] R. Connelly, E. D. Demaine, and G. Rote. Straightening polygonal arcs and convexifying polygonal cycles. *Discrete and Computational Geometry*, 30:205–239, 2003.
- [8] D. Coppersmith and S. Winograd. Matrix multiplication via arithmetic progressions. *J. Symb. Comput.*, 9(3):251–280, 1990.
- [9] H. Crapo and W. Whiteley. Plane self stresses and projected polyhedra I: The basic pattern. *Structural Topology*, 20:55–78, 1993.
- [10] G. Das and M. T. Goodrich. On the complexity of optimization problems for 3-dimensional convex polyhedra and decision trees. *Comput. Geom. Theory Appl.*, 8(3):123–137, 1997.

- [11] H. de Fraysseix, J. Pach, and R. Pollack. How to draw a planar graph on a grid. *Combinatorica*, 10(1):41–51, 1990.
- [12] P. Eades and P. Garvan. Drawing stressed planar graphs in three dimensions. In F.-J. Brandenburg, editor, *Graph Drawing*, volume 1027 of *Lecture Notes in Computer Science*, pages 212–223. Springer, 1995.
- [13] S. J. Gortler, C. Gotsman, and D. Thurston. Discrete one-forms on meshes and applications to 3d mesh parameterization. *Computer Aided Geometric Design*, 23(2):83–112, 2006.
- [14] J. E. Hopcroft and P. J. Kahn. A paradigm for robust geometric algorithms. *Algorithmica*, 7(4):339–380, 1992.
- [15] R. A. Horn and C. R. Johnson. *Matrix Analysis*. Cambridge University Press, 1990.
- [16] M. Lewin. A generalization of the matrix-tree theorem. *Mathematische Zeitschrift*, 181(1):55–70, 1982.
- [17] R. J. Lipton, D. Rose, and R. Tarjan. Generalized nested dissection. *SIAM J. Numer. Anal.*, 16(2):346–358, 1979.
- [18] R. J. Lipton and R. E. Tarjan. Applications of a planar separator theorem. *SIAM J. Comput.*, 9(3):615–627, 1980.
- [19] J. C. Maxwell. On reciprocal figures and diagrams of forces. *Phil. Mag. Ser.*, 27:250–261, 1864.
- [20] S. Onn and B. Sturmfels. A quantitative Steinitz’ theorem. In *Beiträge zur Algebra und Geometrie*, volume 35, pages 125–129, 1994.
- [21] A. Ribó Mor. *Realization and Counting Problems for Planar Structures: Trees and Linkages, Polytopes and Polyominoes*. PhD thesis, Freie Universität Berlin, 2006.
- [22] A. Ribó Mor, G. Rote, and A. Schulz. Embedding 3-polytopes on a small grid. In *SCG’07: Proc. 23rd Annual Symposium on Computational Geometry*, pages 112–118, New York, NY, USA, 2007. ACM.
- [23] A. Ribó Mor, G. Rote, and X. Yong. Upper bounds for the number of spanning trees of a planar graph. in preparation, 2009.
- [24] J. Richter-Gebert. *Realization Spaces of Polytopes*, volume 1643 of *Lecture Notes in Mathematics*. Springer, 1996.
- [25] J. Richter-Gebert and G. M. Ziegler. Realization spaces of 4-polytopes are universal. *Bull. Amer. Math. Soc.*, 32:403, 1995.
- [26] G. Rote. The number of spanning trees in a planar graph. In *Oberwolfach Reports*, volume 2, pages 969–973. European Mathematical Society - Publishing House, 2005.
- [27] W. Schnyder. Embedding planar graphs on the grid. In *Proc. 1st ACM-SIAM Sympos. Discrete Algorithms*, pages 138–148, 1990.
- [28] O. Schramm. Existence and uniqueness of packings with specified combinatorics. *Israel J. Math.*, 73:321–341, 1991.
- [29] A. Schulz. *Lifting Planar Graphs to Realize Integral 3-Polytopes and Topics in Pseudo-Triangulations*. PhD thesis, Freie Universität Berlin, 2008.

- [30] A. Schulz. Drawing 3-polytopes with good vertex resolution. In D. Eppstein and E. R. Gansner, editors, *Graph Drawing*, volume 5849 of *Lecture Notes in Computer Science*, pages 33–44. Springer, 2009.
- [31] E. Steinitz. Polyeder und Raumeinteilungen. In *Encyclopädie der mathematischen Wissenschaften*, volume 3-1-2 (Geometrie), chapter 12, pages 1–139. B. G. Teubner, Leipzig, 1916.
- [32] T. Thiele. Extremalprobleme für Punktmengen. Master’s thesis, Freie Universität Berlin, 1991.
- [33] W. T. Tutte. Convex representations of graphs. *Proceedings London Mathematical Society*, 10(38):304–320, 1960.
- [34] W. T. Tutte. How to draw a graph. *Proceedings London Mathematical Society*, 13(52):743–768, 1963.
- [35] K. Voss and R. Klette. On the maximal number of edges of convex digital polygons included into a square. *Počítače a umelá inteligencia*, 1(6):549–558, 1982. (in Russian).
- [36] W. Whiteley. Motion and stresses of projected polyhedra. *Structural Topology*, 7:13–38, 1982.
- [37] F. Zhang. *Matrix Theory*. Springer, 1999.
- [38] F. Zickfeld. *Geometric and Combinatorial Structures on Graphs*. PhD thesis, Technical University Berlin, December 2007.